Lysophosphatidic Acid Promotes Cell Migration through STIM1- and Orai1-Mediated Ca^{2+}$_i$ Mobilization and NFAT2 Activation

Ralph Jans[1,2], Laura Mottram[1], Darren L. Johnson[1], Anna M. Brown[1], Stephen Sikkink[1], Kehinde Ross[1] and Nick J. Reynolds[1]

Lysophosphatidic acid (LPA) enhances cell migration and promotes wound healing *in vivo*, but the intracellular signaling pathways regulating these processes remain incompletely understood. Here we investigated the involvement of agonist-induced Ca^{2+} entry and STIM1 and Orai1 proteins in regulating nuclear factor of activated T cell (NFAT) signaling and LPA-induced keratinocyte cell motility. As monitored by Fluo-4 imaging, stimulation with 10 μM LPA in 60 μM Ca^{2+}$_o$ evoked Ca^{2+}$_i$ transients owing to store release, whereas addition of LPA in physiological 1.2 mM Ca^{2+}$_o$ triggered store release coupled to extracellular Ca^{2+} entry. Store-operated Ca^{2+} entry (SOCE) was blocked by the SOCE inhibitor diethylstilbestrol (DES), STIM1 silencing using RNA interference (RNAi), and expression of dominant/negative Orai1^{R91W}. LPA induced significant NFAT activation as monitored by nuclear translocation of green fluorescent protein-tagged NFAT2 and a luciferase reporter assay, which was impaired by DES, expression of Orai1^{R91W}, and inhibition of calcineurin using cyclosporin A (CsA). By using chemotactic migration assays, LPA-induced cell motility was significantly impaired by STIM1, CsA, and NFAT2 knockdown using RNAi. These data indicate that in conditions relevant to epidermal wound healing, LPA induces SOCE and NFAT activation through Orai1 channels and promotes cell migration through a calcineurin/NFAT2-dependent pathway.

INTRODUCTION

Lysophosphatidic acid (LPA) is a potent bioactive phospholipid that regulates diverse cellular processes including proliferation, differentiation, adhesion, and migration among several cell types, principally through interaction with a range of specific cell-surface receptors (Noguchi *et al.*, 2009). In the context of wound repair, LPA is released into acute wounds from serum and platelets (Eichholtz *et al.*, 1993; Inoue *et al.*, 1995; Goetzl and An, 1998; Baker *et al.*, 2002; Mazereeuw-Hautier *et al.*, 2005) and is present in physiologically relevant concentrations in blister fluid (Mazereeuw-Hautier *et al.*, 2005). LPA has been shown to promote migration of cultured epidermal keratinocytes (Sauer *et al.*, 2004) and to enhance wound closure following topical application to experimental wounds in rats and mice (Demoyer *et al.*, 2000; Balazs *et al.*, 2001). LPA-induced signaling is complex and involves the activation of specific G protein–coupled receptors (LPA$_{1–6}$), as well as transactivation of other plasma membrane receptors (Sekharam *et al.*, 2000; Sauer *et al.*, 2004; Noguchi *et al.*, 2009). Binding of LPA to its specific receptors also elicits mobilization of intracellular calcium (Ca^{2+}$_i$) from IP$_3$-dependent stores and influx of extracellular Ca^{2+} (Ca^{2+}$_o$) mediated by incompletely defined mechanisms (Noguchi *et al.*, 2009). Keratinocytes are known to express LPA$_{1–3}$ and respond to LPA with Ca^{2+} transients (Anliker and Chun, 2004; Roedding *et al.*, 2006; Ross *et al.*, 2007; Lichte *et al.*, 2008), but the physiological relevance of LPA-induced Ca^{2+} fluxes and the downstream signaling pathways in mediating specific physiological effects remain to be defined.

Recent studies have identified the endoplasmic reticulum Ca^{2+} sensor STIM1 and the plasma membrane channel protein Orai1 as critical components of agonist-induced Ca^{2+} entry (Frischauf *et al.*, 2008; Martin *et al.*, 2009), as well as being crucial for tumor cell migration (Vassilieva *et al.*, 2008; Yang *et al.*, 2009; Zuo and Chen, 2009). Our previous data suggested a role for STIM1 in mediating Ca^{2+} entry in keratinocytes (Ross *et al.*, 2007, 2008), but there is currently no information regarding the role of STIM1 or Orai1 in regulating keratinocyte migration.

[1]*Dermatological Sciences, Institute of Cellular Medicine, Newcastle University, Newcastle upon Tyne, UK*

[2]*Current address: Cardio3 Biosciences, 12 Rue Edouard Belin, B-1435 Mont-Saint-Guibert, Belgium*

Correspondence: Nick J. Reynolds, Dermatological Sciences, Institute of Cellular Medicine, Newcastle University, Framlington Place, Newcastle upon Tyne NE2 4HH, UK. E-mail: n.j.reynolds@ncl.ac.uk

The calcineurin/nuclear factor of activated T cell (NFAT) signaling cascade is characteristically recruited by the sustained Ca^{2+}_i mobilization observed during Ca^{2+} entry (Macian, 2005; Gwack *et al.*, 2007). NFAT factors have been determined to be crucial for regulating cell motility in several cell types (Jauliac *et al.*, 2002; Corral *et al.*, 2007). We and others have shown that NFAT factors are functionally active in keratinocytes and epidermis, and calcineurin/NFAT activity has also been directly implicated in the regulation of keratinocyte growth and differentiation (Santini *et al.*, 2001; Al-Daraji *et al.*, 2002; Mammucari *et al.*, 2005). The relationship between Ca^{2+} fluxes and NFAT activation in keratinocytes remains to be determined, and furthermore, the involvement of calcineurin/NFAT signaling in LPA-induced cell motility remains unknown.

In this study, we therefore investigated the hypothesis that LPA promotes keratinocyte migration through Ca^{2+}_i mobilization and examined the role of STIM1, Orai1 and calcineurin/NFAT recruitment within these physiological phenomena.

RESULTS

Stimulation of keratinocytes with LPA in physiological Ca^{2+}_o triggers Ca^{2+} entry

As previous studies in lymphocytes have indicated that sustained increases in Ca^{2+}_i encountered during Ca^{2+} entry (Gwack *et al.*, 2007) are required for NFAT activation (Dolmetsch *et al.*, 1997), we first determined the experimental conditions in which LPA could evoke Ca^{2+} entry in primary keratinocytes. LPA is known to induce short transient elevations of Ca^{2+}_i due to the release of Ca^{2+} from intracellular stores, but Ca^{2+} entry has not been reported (Ross *et al.*, 2007, 2008; Lichte *et al.*, 2008). As the relevance of Ca^{2+}_o in the regulation of LPA-induced Ca^{2+} mobilization in keratinocytes has largely been ignored, we investigated LPA-induced Ca^{2+} mobilization in the context of varying Ca^{2+}_o.

Keratinocytes were routinely cultured in medium containing 60 µM Ca^{2+}_o. The addition of 10 µM LPA in these conditions induces a transient (± 200 seconds) peak elevation of Ca^{2+}_i (Figure 1a), indicative of store release as expected (Ross *et al.*, 2007, 2008; Lichte *et al.*, 2008). Adjustment of the Ca^{2+}_o to 1.2 mM in the absence of LPA resulted in a weak increase in Ca^{2+}_i (Figure 1a) over an extended period of time (>10 minutes), similar to previous reports (Bikle *et al.*, 1996; Tu *et al.*, 2001). To mimic the contact of keratinocytes with LPA in a serum-relevant Ca^{2+}_o, we analyzed the effect of adding LPA in 1.2 mM Ca^{2+}_o. Under these conditions, LPA induced a transient peak in Ca^{2+}_i, followed by a sustained (>10 minutes) plateau elevation of Ca^{2+}, which suggests store release coupled to entry of extracellular Ca^{2+} (Figure 1a).

We then used an addback protocol to verify the occurrence of Ca^{2+} entry by uncoupling store release from influx (Figure 1b). Manganese quenching (Sage *et al.*, 1989) by the addition of 500 µM $MnCl_2$ during the plateau phase quickly reduced Ca^{2+}_i to the baseline level (Figure 1b). In addition, we used Ca^{2+} entry–blocking pharmacological agents to further define the Ca^{2+}-mobilizing effect of LPA. We initially validated the pharmacological agents through studies on

thapsigargin (Tg)-induced Ca^{2+} entry. Although 2-aminoethoxydiphenyl borate has been classically used to block store-operated Ca^{2+} entry (SOCE), this molecule is increasingly recognized to be rather nonspecific (Schindl *et al.*, 2008). We found that 2-aminoethoxydiphenyl borate did not block Tg-induced Ca^{2+} entry at a variety of concentrations (data not shown). Similarly, we found that the addition of gadolinium ions (Gd^{3+}) did not reliably block Tg-induced SOCE (data not shown). We therefore used the lesser known SOCE inhibitor diethylstilbestrol (DES), which blocks SOCE channels and inwardly rectifying current but exerts no effect on TRPM channels (Zakharov *et al.*, 2004; Dobrydneva *et al.*, 2010). DES was indeed found to inhibit Tg-induced SOCE in keratinocytes (Figure 1c), and the addition of DES during the plateau phase of LPA-induced Ca^{2+} entry blocked further entry (Figure 1b), providing further evidence that LPA induces Ca^{2+} entry in keratinocytes through SOCE channels.

To further characterize the impact of Ca^{2+}_o on LPA-induced Ca^{2+} mobilization, keratinocytes were incubated in medium containing 1.2 mM Ca^{2+} for an extended time (45 minutes) before LPA stimulation. Under these conditions, LPA induced store release (Figure 1d) in a manner similar to previous studies (Ross *et al.*, 2007; Lichte *et al.*, 2008), but no entry was apparent during the observed time span (>10 minutes). Next, we uncoupled the addition of agonist and Ca^{2+} by adjusting the Ca^{2+}_o to 1.2 mM for 60 seconds before adding LPA (Roedding *et al.*, 2006) (Figure 1e). There was no significant difference detected between Ca^{2+}_i fluxes observed in these conditions and when LPA and millimolar Ca^{2+} were added simultaneously, suggesting that simultaneous stimulation of LPA receptors and adjustment to millimolar Ca^{2+} does not just overwhelm the plasma membrane channels and thereby cause nonspecific entry.

LPA induces nuclear translocation of NFAT2 and upregulates NFAT transcriptional activity

We then investigated the effect of LPA on NFAT activation. First, we used a real-time live-cell imaging method to simultaneously analyze Ca^{2+}_i variations (using FuraRed) and NFAT activation (by visualizing nuclear translocation of green fluorescent protein (GFP)-tagged NFAT2). The proof-of-principle of this method was achieved by triggering Tg-mediated SOCE, which resulted in a sustained Ca^{2+}_i increase as expected. This correlated with progressive and strong nuclear accumulation of NFAT2-GFP within 10 minutes of exposure (Figure 2a).

Simultaneous stimulation with LPA and 1.2 mM Ca^{2+}_o resulted, as expected, in Ca^{2+} store release coupled to entry, which correlated with progressively increasing nuclear accumulation of NFAT2 (Figure 2b). Adjustment of Ca^{2+}_o to 1.2 mM did not induce significant NFAT2 translocation within 10 minutes of treatment (Figure 2c). In all experimental conditions, nuclear translocation of NFAT2 was prevented by preincubating the cells for 1 hour with the calcineurin inhibitor cyclosporin A (CsA, 1 µM) before agonist challenge (data not shown).

Second, we investigated the effect of LPA on NFAT activity using a luciferase reporter under the transcriptional control of
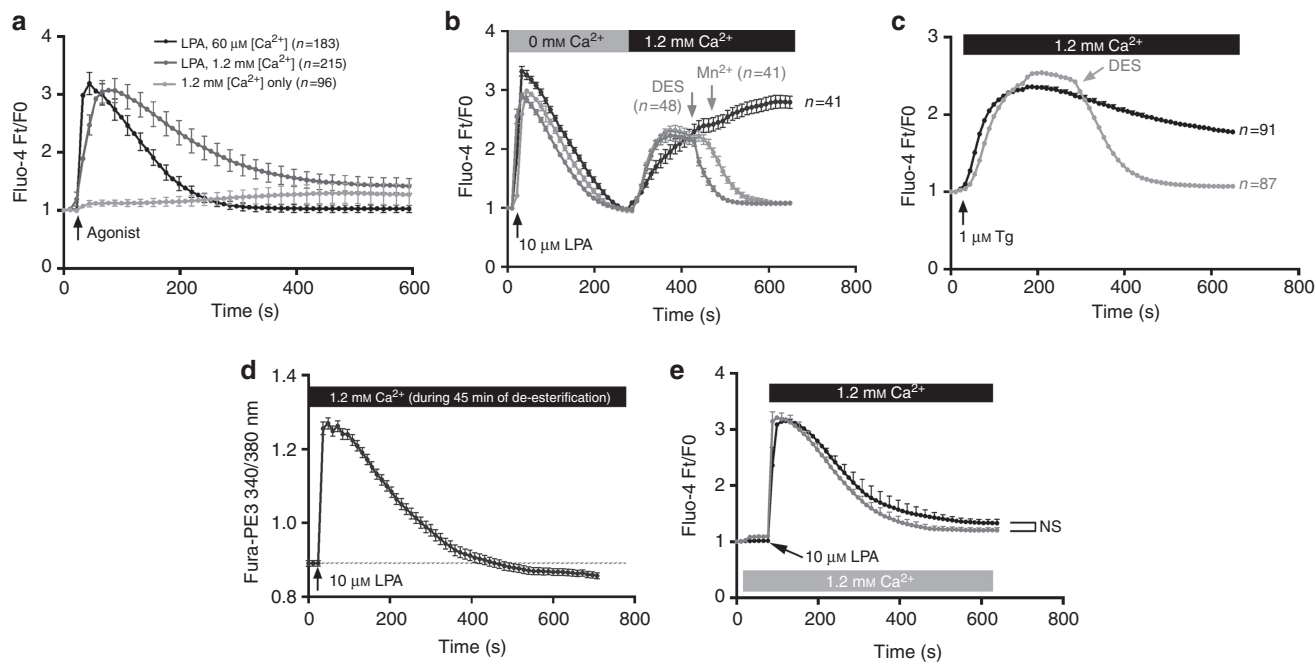
Figure 1. Lysophosphatidic acid (LPA) stimulation in 1.2 mM Ca^{2+}_o evokes Ca^{2+} entry. Keratinocytes were subjected to Ca^{2+}_i imaging. (**a**) Stimulation with 10 μM LPA in 60 μM or 1.2 mM Ca^{2+}_o or with 1.2 mM Ca^{2+}_o. (**b**) Uncoupling of store release and entry using LPA in Ca^{2+}-free medium and adding back Ca^{2+}. Ca^{2+} entry was blocked by the addition of 500 μM $MnCl_2$ or 10 μM DES. (**c**) Thapsigargin (Tg)-induced store-operated Ca^{2+} entry was inhibited by adding diethylstilbestrol (DES). (**d**) LPA added after exposure to Ca^{2+}_o during de-esterification (45 minutes, $n=49$) caused only store release. (**e**) Cells were exposed to 1.2 mM Ca^{2+}_o for 60 seconds before LPA (gray, $n=134$) or LPA was added in 1.2 mM Ca^{2+}_o ($n=83$). No significant difference in Ca^{2+} entry was observed (two-way analysis of variance at $t=600$ seconds).

NFAT (Wilkins *et al.*, 2004). LPA stimulation in 1.2 mM Ca^{2+}_o prompted a significant and sustained upregulation of NFAT activity to a level ~10-fold over baseline within 4 hours after stimulation (Figure 3a). In comparison, LPA stimulation in 60 μM Ca^{2+}_o increased NFAT activity within 4 hours before reaching a plateau level ~2.5-fold over the control level (Figure 3a). Adjustment of Ca^{2+}_o to 1.2 mM in the absence of LPA induced a weak increase of NFAT activity (~2.5-fold) over 24 hours (Figure 3a). As shown in Figure 3b, preincubation of keratinocytes for 1 hour with 1 μM CsA before LPA and millimolar Ca^{2+}_o challenge prevented the induction of NFAT transcriptional activity. To further investigate the role of Ca^{2+} entry in LPA-induced NFAT activation, DES was added during agonist challenge, which resulted in a significantly impaired induction of NFAT activity (Figure 3c).

Characterization of the mechanism of LPA-induced Ca^{2+} entry
The implication of STIM1 in LPA-induced Ca^{2+} entry was studied by analyzing the effect of RNA interference (RNAi-mediated) knockdown of STIM1 expression using nucleofection, which achieves efficient transfection of primary keratinocytes (Supplementary Figure S1 online). Figure 4a–c illustrates that keratinocytes transfected with small interfering RNA (siRNA) directed against STIM1 exhibit a significant decrease in STIM1 mRNA and protein content 24 hours post transfection. Figure 4d shows that LPA-induced Ca^{2+} entry was impaired in STIM1 siRNA-transfected keratinocytes compared with scrambled siRNA-transfected cells.

The involvement of Orai1 in LPA-induced Ca^{2+} influx was investigated by evaluating the impact of overexpressing $Orai1^{R91W}$, an Orai1 mutant that substantially attenuates Ca^{2+} entry through Orai1 channels through a dominant-negative effect (Liao *et al.*, 2007). Figure 4e and f illustrates efficient transfection of Orai1-encoding plasmids to keratinocytes by nucleofection. As shown in Figure 4g, LPA-induced Ca^{2+} influx was inhibited in $Orai1^{R91W}$-expressing keratinocytes, whereas entry levels were comparable in wild-type Orai1-expressing and empty vector–transfected cells. Notably, subsequent LPA-induced upregulation of NFAT transcriptional activity was found to be impaired in $Orai1^{R91W}$-expressing cells, but not in wild-type Orai1- or empty vector–transfected cells (Figure 4h). A similar effect was observed following siRNA-mediated knockdown of Orai1 (Supplementary Figure S2 online).

LPA-induced keratinocyte migration requires STIM1, calcineurin, and NFAT2
To test the involvement of STIM1 in mediating LPA-induced keratinocyte migration, keratinocytes were subjected to STIM1 knockdown before performing three-dimensional (3D) chemotactic migration assays. Cells were allowed to migrate over 14 hours in medium containing 60 μM Ca^{2+} or 1.2 mM Ca^{2+} to mimic the contact of keratinocytes with LPA in high Ca^{2+}_o, as would occur following wounding of skin. As described previously, exposure to millimolar Ca^{2+}_o dampened overall migration rates (Figure 5a and b) (Magee *et al.*, 1987). In both Ca^{2+}_o conditions, LPA treatment induced a significant increase in keratinocyte motility, as expected (Sauer *et al.*,
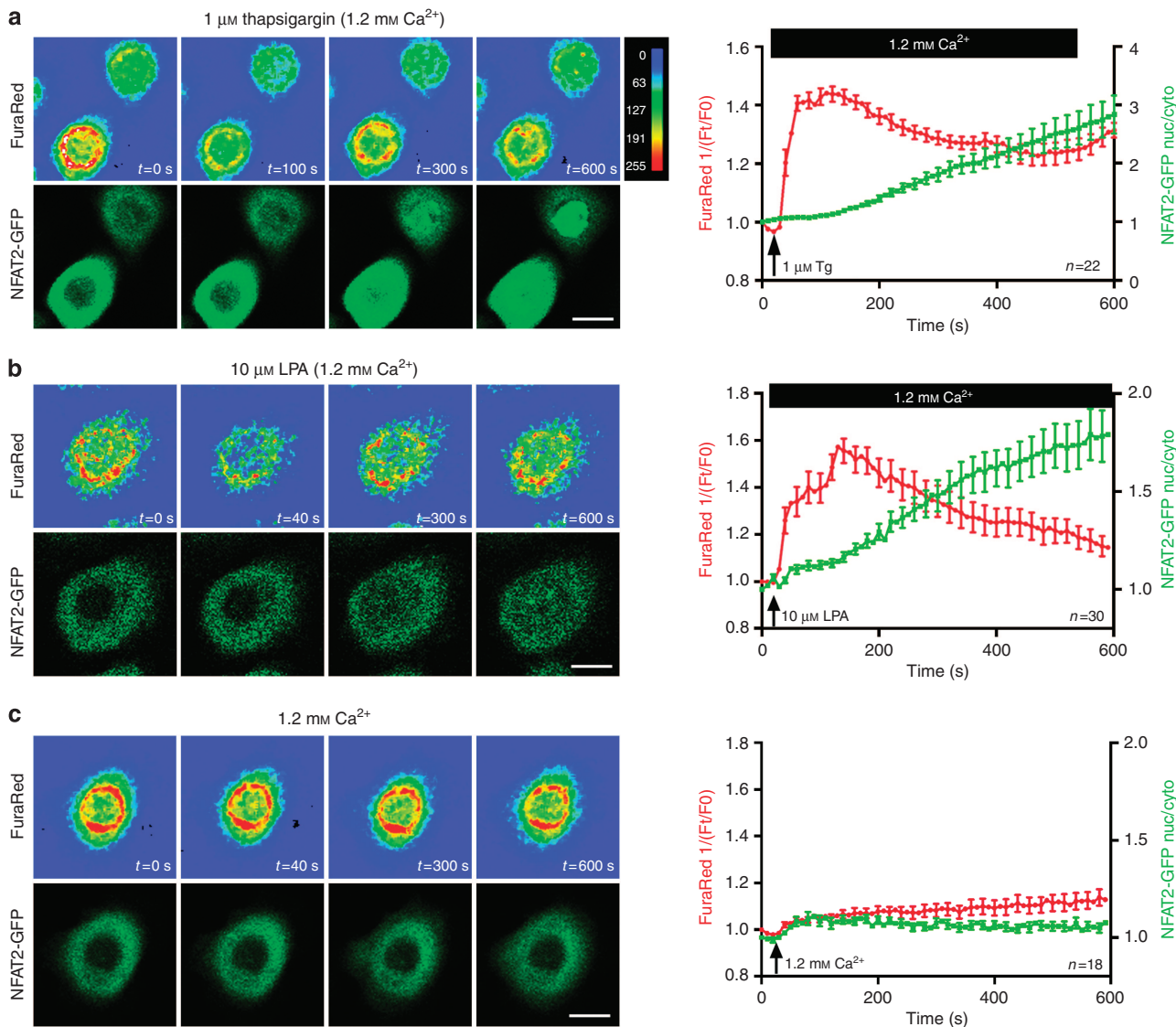
Figure 2. LPA-induced Ca^{2+} mobilization correlates with nuclear translocation of GFP-tagged nuclear factor of activated T cell 2 (NFAT2). Keratinocytes expressing green fluorescent protein (GFP)-tagged NFAT2 were subjected to Ca^{2+}_i imaging using FuraRed. Ca^{2+}_i variations are indicated as $1/(F_t/F_0)$ (red data points), whereas the ratio of nuclear versus cytoplasmic localization of NFAT2-GFP is represented by green data points $\pm$ SEM in histograms. Representative FuraRed and NFAT2-GFP snapshots are shown for illustration purposes. (**a**) For proof-of-principle, store-operated Ca^{2+} entry was induced using 1 μM thapsigargin in 1.2 mM Ca^{2+}_o. (**b**) Stimulating the cells with 10 μM lysophosphatidic acid (LPA) in 1.2 mM Ca^{2+}_o resulted in store release and influx correlating with NFAT2 translocation. (**c**) Adjusting Ca^{2+}_o to 1.2 mM did not trigger noticeable NFAT2 translocation. Bar = 10 μm.

2004). However, LPA-induced migration was significantly impaired in the 3D assays (Figure 5b) following STIM1 knockdown, suggesting that normal levels of STIM1 are required for LPA-induced keratinocyte motility.

To investigate the involvement of the calcineurin/NFAT pathway in mediating LPA-induced migration, cells were pretreated using the calcineurin inhibitor CsA before being subjected to two-dimensional scratch wounding (Supplementary Figure S3 online) and 3D chemotactic migration assays (Figure 5c and d). LPA-induced migration was significantly impaired in CsA-treated keratinocytes. Moreover, RNAi-mediated knockdown of NFAT2, the efficiency of which was verified by real-time PCR (Figure 5e) and western blotting

(Figure 5f and g), significantly prevented the induction of 3D migration of keratinocytes by LPA in 60 μM and 1.2 mM Ca^{2+}_o (Figure 5h and i).

DISCUSSION

The data presented in this paper (schematically summarized in Figure 6) demonstrate that stimulation of keratinocytes with LPA induces Ca^{2+}_o-regulated mobilization of Ca^{2+}_i, leading to the activation of calcineurin/NFAT2 signaling and keratinocyte migration. LPA stimulation in physiological millimolar Ca^{2+}_o evoked agonist-induced Ca^{2+} entry, which required sufficient levels of STIM1 and functional Orai1. Downstream of LPA-induced Ca^{2+} mobilization, we observed nuclear
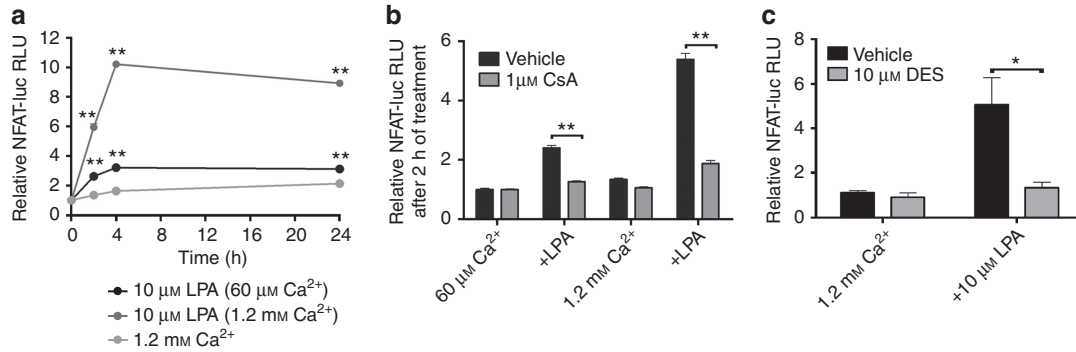
Figure 3. Lysophosphatidic acid (LPA)-induced Ca^{2+} entry triggers sustained calcineurin-dependent upregulation of nuclear factor of activated T cell (NFAT) transcriptional activity. (**a**) Keratinocytes were stimulated as indicated and assessed for NFAT-dependent luciferase activity expressed as mean ± SEM. (**b**, **c**) Calcineurin activity (**b**) and Ca^{2+} entry (**c**) were required for LPA-induced NFAT activation (*$P<0.05$, **$P<0.01$, one-way analysis of variance).
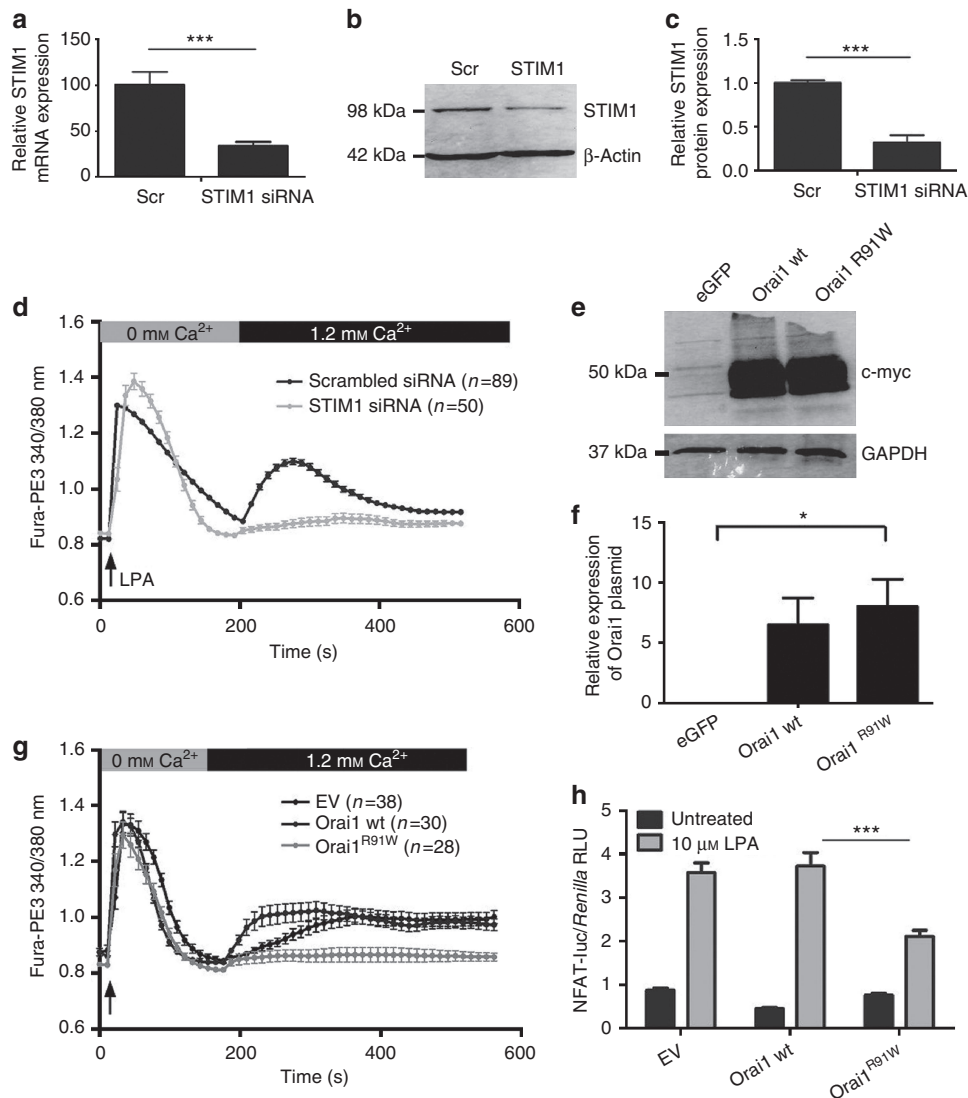

Figure 4. Lysophosphatidic acid (LPA)-induced Ca^{2+} entry requires sufficient levels of STIM1 and functional Orai1. (**a**–**c**) Relative efficiency of small interfering RNA (siRNA)-mediated STIM1 silencing compared to scrambled (scr) control by quantitative PCR and western blotting. (**e**) Fura-PE3-based Ca^{2+} imaging showed impaired LPA-induced Ca^{2+} entry in STIM1-knockdown cells. (**e**, **f**) Efficient transfection of Orai1-encoding plasmids demonstrated by western blotting for myc-tag. (**g**) LPA-induced Ca^{2+} entry was found to be blocked in $Orai1^{R91W}$-expressing cells. (**h**) Keratinocytes were cotransfected with Orai1, nuclear factor of activated T cell (NFAT)-directed, and *Renilla* luciferase plasmids. Cells were then treated with LPA and 1.2 mM Ca^{2+} and assessed for NFAT transcriptional activity. Overexpression of $Orai1^{R91W}$ significantly impaired NFAT activation. Data represent mean ± SEM; $n \geqslant 3$ unless otherwise stated, *$P<0.05$, **$P<0.01$, ***$P<0.001$, analysis of variance.
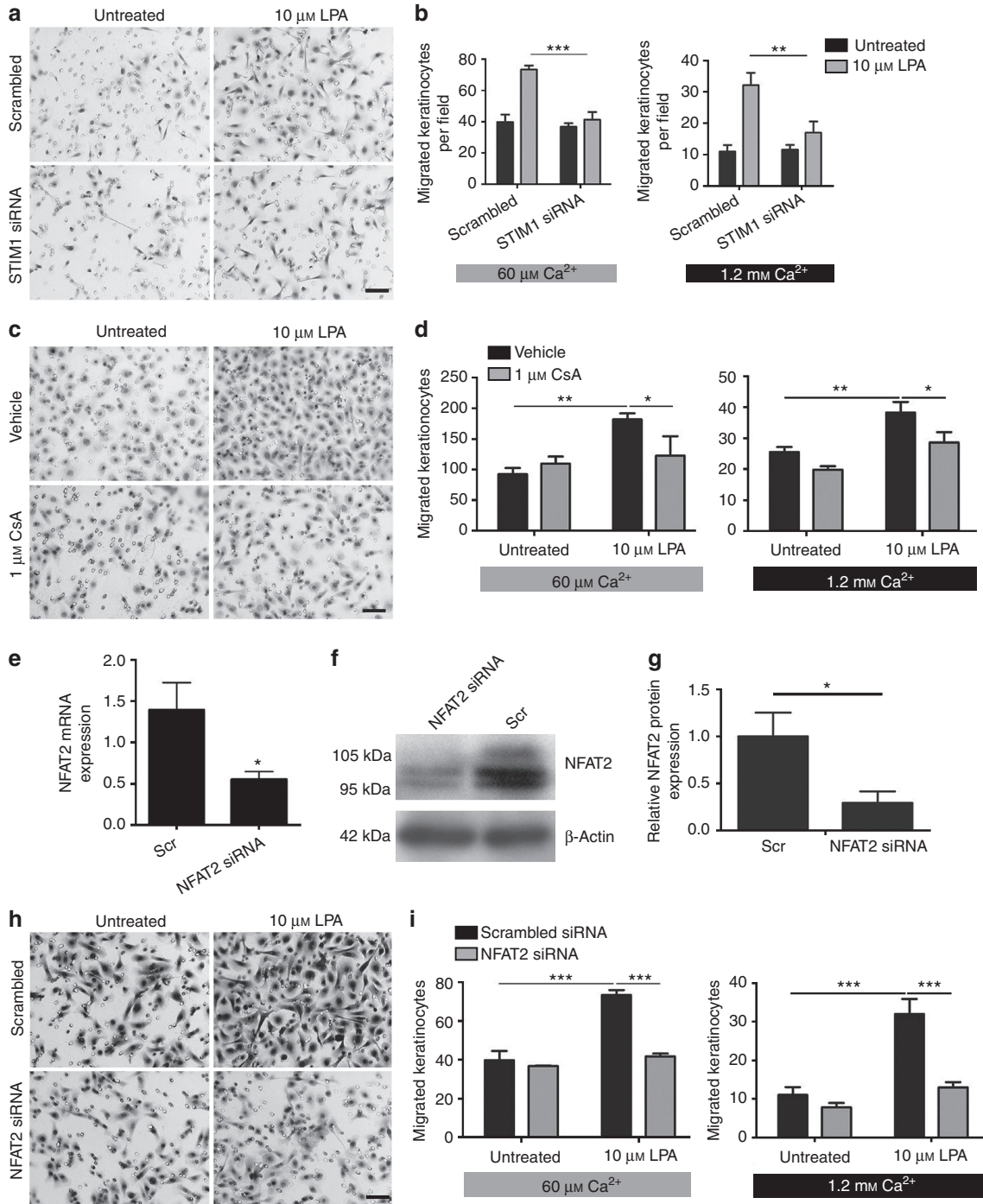
Figure 5. Lysophosphatidic acid (LPA)-induced keratinocyte migration requires STIM1, calcineurin activity, and sufficient levels of nuclear factor of activated T cell 2 (NFAT2). (a–d, h, i) Keratinocyte cultures were subjected to three-dimensional (3D) chemotactic migration assays, which were performed in medium containing 60 μM or 1.2 mM Ca^{2+}. The average numbers of migrated cells are represented as bar graphs ± SEM. Keratinocytes were treated with scrambled (scr) or STIM1-targeted small interfering RNA (siRNA) (a, b) or NFAT2-targeted siRNA (h, i) for 24 hours prior to 3D chemotactic migration assays. In both Ca^{2+} conditions, 10 μM LPA significantly increased migration rates. RNA interference (RNAi)-mediated knockdown of STIM1 and NFAT2 resulted in a significant impairment of LPA-induced keratinocyte motility (a, b, h, i, ***$P<0.001$, **$P<0.01$, two-way analysis of variance (ANOVA)). (c, d) Preincubation of cells with 1 μM cyclosporin A significantly impaired LPA-induced migration ($n\geqslant3$, **$P<0.01$, *$P<0.05$, two-way ANOVA). (e–g) Keratinocytes were transfected using scr or NFAT2-targeted siRNA. After 24 hours, cells were subjected to (e) real-time PCR analysis of NFAT2 expression ($n=6$), (f) western blot analysis, and (g) densitometry ($n=3$). RNAi-mediated knockdown of NFAT2 is significant (*$P<0.05$, t-test). Bar = 50 μm.
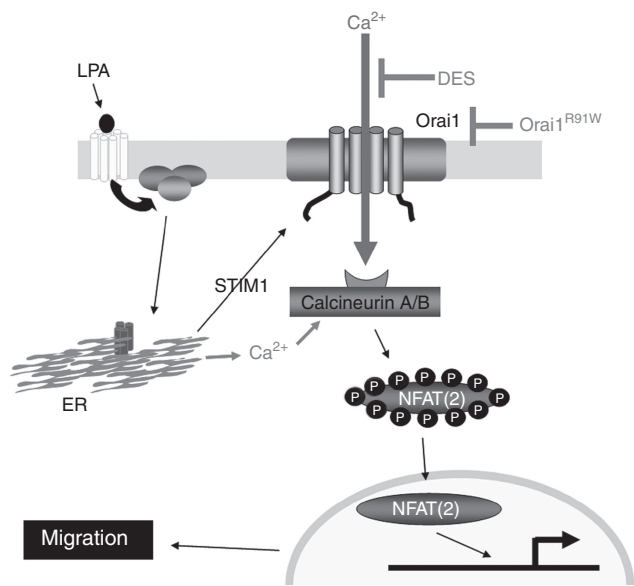
Figure 6. Proposed mechanism of lysophosphatidic acid (LPA)-induced Ca^{2+} signaling involved in promoting keratinocyte migration. On the basis of our results, this model proposes that in physiological conditions, LPA promotes migration of keratinocytes through Ca^{2+} mobilization mediated by STIM1 and Orai1 and subsequent activation of calcineurin and nuclear factor of activated T cell 2 (NFAT2). ER, endoplasmic reticulum.

translocation of NFAT2 and activation of NFAT-dependent transcription. Finally, LPA-induced keratinocyte motility required sufficient levels of STIM1 and NFAT2 and calcineurin activity. Our study thus provides important insight into the signaling mechanism triggered by LPA to promote keratinocyte migration.

The physiology of keratinocytes is well known to be tightly regulated by Ca^{2+}_o (Tu *et al.*, 2004). Consistent with this, our data show differential Ca^{2+} mobilization and NFAT activation upon stimulation with LPA in physiological millimolar Ca^{2+}_o compared with micromolar levels. Indeed, LPA induced Ca^{2+} entry when the Ca^{2+}_o was adjusted to 1.2 mM simultaneously with or briefly before stimulation. However, keratinocytes left in 1.2 mM Ca^{2+}_o for a prolonged time before LPA stimulation only exhibited store release, but no Ca^{2+} entry was detectable within the observed time span, which is in accordance with previous studies (Ross *et al.*, 2007, 2008; Lichte *et al.*, 2008) and suggests that prolonged exposure to millimolar Ca^{2+} results in the inhibition of acute LPA-induced Ca^{2+} entry. Our data indicating NFAT activation caused by Ca^{2+} entry are consistent with previous studies performed in other epithelial cell types, including prostate (Thebault *et al.*, 2006) and kidney (Schlondorff *et al.*, 2009) cells.

The role of store- and receptor-operated Ca^{2+} entry (SOCE/ ROCE) during physiological activation of primary cells has not been extensively investigated, and thus there is little information on the roles of STIM and Orai proteins in primary cells except in hepatocytes, in which STIM1 and Orai1 are involved in mediating Ca^{2+} entry leading to agonist-induced oscillations (Jones *et al.*, 2008). To our knowledge, the establishment

of functional roles for STIM1 and Orai1 in primary keratinocytes as mediators of agonist-induced Ca^{2+} entry has previously been unreported. Our data showing that LPA-induced Ca^{2+} entry depends on normal levels of STIM1 and functional Orai1 are consistent with studies in which STIM1 knockdown (Hirano *et al.*, 2009; Potier *et al.*, 2009) and expression of dominant/negative Orai1[R91W] (Liao *et al.*, 2007, 2008) lead to the inhibition of SOCE or ROCE in a variety of cell lines.

Our data concur with an increasing body of evidence indicating an emerging role for Ca^{2+} signaling as a critical regulator of cell motility in a variety of physiological and pathological contexts. For instance, STIM1 and Orai1 have been found to mediate agonist-induced Ca^{2+} entry and regulate Ca^{2+} flux–dependent cell migration in epithelial tumor cells (Yang *et al.*, 2009) and vascular smooth muscle cells (Potier *et al.*, 2009). In addition, functional inhibition of calcineurin and NFAT2 impaired the migration rate of epithelial tumor cells (Jauliac *et al.*, 2002), and wound closure in scratched myocyte cultures was reduced by silencing NFAT2 expression (Chow *et al.*, 2008).

NFAT transcription factors have been previously attributed to important roles in the control of keratinocyte growth and differentiation (Santini *et al.*, 2001; Mammucari *et al.*, 2005; Horsley *et al.*, 2008) and in the response of keratinocytes to UV-mediated stress (Canning *et al.*, 2006; Flockhart *et al.*, 2008). In conclusion, our work underscores the importance of Ca^{2+} signaling and NFAT factors in the control of epidermal physiology and potentially in cutaneous wound healing.

MATERIALS AND METHODS
Reagents
All chemicals were purchased from Sigma-Aldrich (Gillingham, UK) unless otherwise specified.

Cell culture and treatments
Normal human epidermal keratinocytes were isolated from redundant foreskins (Todd and Reynolds, 1998) or breast or abdominal skin (Jans *et al.*, 2004), and primary cultures were expanded in human keratinocyte growth supplement EpiLife medium (Invitrogen, Paisley, UK). The study adhered to the Declaration of Helsinki protocols for use of human materials, was approved by the Newcastle and North Tyneside local ethics committee, and written informed patient consent was obtained. Keratinocytes were used between passage 2 and 5. Treatments with agonists were performed by diluting the agonists directly in medium. For inhibition of calcineurin activity, cells were pretreated with 1 μM CsA (Calbiochem, San Diego, CA) for 1 hour before agonist challenge. The concentration of LPA used throughout the study was 10 μM, which is a generally accepted concentration (Ross *et al.*, 2007, 2008; Lichte *et al.*, 2008).

Ca^{2+} imaging
Keratinocytes seeded in Willco glass-bottomed dishes (Intracel, Royston, UK) were subjected to Ca^{2+}_i imaging using Fluo-4-AM (Invitrogen) or Fura-PE3-AM (Calbiochem) as described (Ross *et al.*, 2007). Changes in Ca^{2+}_i were monitored at 10-second intervals with a Pathway HTS imaging system (Becton-Dickinson, Rockville, MD).

Images were captured using an Olympus (Melville, NY) $\times 20$ objective and a Hamamatsu 1394 (Hamamatsu, Japan) ORCA-ERA CCD camera. Fluo-4 was excited at 488 nm, collecting emitted fluorescence through a 515LP filter. Fura-PE3 was excited at 340 and 380 nm, and emitted fluorescence was collected through the 515LP filter. Quantification was performed using Volocity (Improvision, Coventry, UK). When using Fluo-4, changes in Ca^{2+}_i are expressed as the ratio of the initial fluorescence to the temporal fluorescence (F_t/F_0). When using Fura-PE3, changes in Ca^{2+}_i are expressed as ratiometric measurements (F_{340nm}/F_{380nm}).

Dual imaging of Ca^{2+}_i and NFAT2-GFP

Keratinocytes transduced with NFAT2-GFP-delivering retroviruses (Flockhart *et al.*, 2008) were seeded on Willco dishes. After 24 hours, the cells were loaded using 5 μM FuraRed-AM (Invitrogen). Dual imaging was then performed using a Leica TCS SP2 confocal laser scanning microscope equipped with an argon laser (Leica, Milton Keynes, UK). Fluorescence excitation of GFP and FuraRed was performed with the 488-nm line of the laser. Fluorescence emission of GFP was collected through a 500–550-nm window of the detector, whereas FuraRed emission was collected through a 650–700-nm window. Images were captured with a $\times 63$ Plan Apo objective (NA1.32) (Leica, Milton Keynes, UK) at 10-second intervals. Changes in Ca^{2+}_i are expressed as the inverted ratio of the initial fluorescence to the temporal fluorescence ($1/(F_t/F_0)$). The nuclear-to-cytoplasmic ratio of NFAT2-GFP was assessed by outlining the nucleus and cytoplasm of each cell as separate region of interest, calculating the mean green fluorescence in each regions of interest and frame in Volocity. Nuclear-to-cytoplasmic ratios were then calculated in Microsoft Excel.

NFAT transcriptional activity assay

NFAT transcriptional activity was measured using an NFAT firefly luciferase reporter plasmid (pGL3; Promega, Southampton, UK), containing nine copies of an NFAT-binding site from the IL-4 promoter (5′-TGGAAAATT-3′) positioned 5′ to a minimal promoter from the α-myosin heavy-chain gene, gratefully obtained from J Molkentin, Cincinnati, OH (Wilkins *et al.*, 2004). Transfection efficiency and cell viability were controlled by cotransfecting a *Renilla* luciferase control vector (pRLTK; Promega). Keratinocytes were seeded in 12-well plates and transfected using 0.5 μg of firefly reporter DNA plus 0.05 μg of *Renilla* luciferase DNA using Fugene 6 (Roche Applied Sciences, Burgess Hill, UK) at a 6:1 Fugene:DNA ratio. After 24 hours, the cells were stimulated as indicated, lysed, and assayed for dual luciferase activity. Luciferase assays were performed using the dual luciferase assay system (Promega). Reporter firefly luciferase values were normalized to the *Renilla* values.

RNA interference to knock down STIM1 and NFAT2 expression

Chemically modified (to prevent off-target effects) scrambled siRNA and NFAT2-specific siRNA were obtained from Qiagen (Crawley, UK) (Flockhart *et al.*, 2009). STIM1-targeted siRNA (5′-GAAGCC UCUUAAGAAGUAG-3′ and 5′-AGACCUCAAUUACCAUGAC-3′) was obtained from Eurofins/MWG (Ebersberg, Germany). siRNA was transfected into keratinocytes using the Human Keratinocyte Nucleofector kit and device from Amaxa/Lonza (Cologne, Germany) according to the manufacturer's protocol (2 μg siRNA per 10^6 cells).

For STIM1, 1 μg of each siRNA was used to transfect 10^6 cells. After 24 hours, the cells were trypsinized and subjected to the 3D chemotactic migration assay. Knockdown of STIM1 and NFAT2 was verified by real-time PCR and western blotting using standard techniques (Hampton *et al.*, 2012) and anti-STIM1 antibody (clone 5A2; Abnova, Taipei, Taiwan) or anti-NFAT2 antibody (a kind gift from Dr Nancy Rice) (Hampton *et al.*, 2012), respectively. For NFAT2 real time, Poly-A RNA was isolated using a Direct mRNA isolation kit (Sigma-Aldrich, Gillingham, UK), retrotranscribed using a High-Capacity cDNA RT kit (Applied Biosystems, Paisley, UK) and subjected to real-time PCR using iQ SYBR Green Supermix and a Chromo4 cycler (Bio-Rad, Hemel Hempstead, UK). Primers used to detect NFAT2 were 5′-CTTCTCCAACACCAAAGTCC-3′ (forward) and 5′-CGTACCCGTGTGTTCTTCCT-3′ (reverse). NFAT2 expression was normalized to glyceraldehyde-3-phosphate dehydrogenase expression (forward primer: 5′-GTCAGTGGTGGACCTGACCT-3′ and reverse primer: 5′-AGGGGTCTACATGGCAACTG-3′). For STIM1 real time, total RNA was isolated using the Arcturus PicoPure RNA Isolation kit (Applied Biosystems) and reverse transcribed using the SuperScript III First-Strand Synthesis System (Invitrogen); TaqMan gene-expression assays Hs00162394_m1 (STIM1) and Hs99999905_m1 (glyceraldehyde-3-phosphate dehydrogenase) (Applied Biosystems) were performed on a 7900HT system (Applied Biosystems).

Effect of dominant/negative Orai1^{R91W} on LPA-induced Ca^{2+} entry

pCMV-myc plasmids encoding wild-type Orai1 or mutated dominant/negative Orai1^{R91W} were kindly donated by Professor L Birnbaumer (Liao *et al.*, 2007) (NIEHS, Research Triangle Park, NC). Keratinocytes (10^6 cells) were transfected by nucleofection with 2 μg of Orai1-encoding plasmid and 0.5 μg of pEGFP-N1 (Clontech, Mountain View, CA) to mark the transfected cells (Zarayskiy *et al.*, 2007). The expression of myc-tagged Orai1-encoding plasmids was verified by standard western blotting using anti-myc antibody (clone 9E10; Santa Cruz Biotechnology, San Diego, CA). Cells were seeded into Willco dishes at 0.5×10^6 cells per dish. After 24 hours, the cells were processed for Ca^{2+}_i imaging using Fura-PE3. Before performing Ca^{2+} imaging, the sample field was analyzed for GFP expression using the appropriate filter sets.

Migration assays

Keratinocyte motility was assessed using standard two-dimensional scratch wounding and 3D chemotactic migration assays. Chemotactic migration of keratinocytes was assayed in a manner similar to that described in Sauer *et al.*, 2004. Briefly, 20,000 keratinocytes were seeded on top of uncoated Transwell filters (12 mm diameter, 8 μm pore size; Corning Life Sciences, Schiphol-Rijk, The Netherlands) in a 10-μl drop. Care was taken to deposit the drop in the middle of the filter without it touching the plastic support walls, in order to prevent a meniscus effect causing unequal distribution. The cells were left to attach for 30 minutes at room temperature before adding 300 μl of EpiLife medium containing agonists into the lower compartment. The cells were left to migrate overnight at 37 °C before fixation using 4% (w/v) formaldehyde. Unmigrated cells were scraped off the top portion of the filters using cotton buds. The filters were stained using hematoxylin and eosin, cut out and mounted using DPX. The migrated cells were counted on a Leica photomicroscope using a $\times 10$ objective (3–5 fields per sample).

Statistical analysis

Statistical analysis was performed using Prism 5 (GraphPad Software, San Diego, CA). Data represent mean ± SEM. Experiments were repeated at least three times using different keratinocyte strains unless otherwise specified.

SUPPLEMENTARY MATERIAL

Supplementary material is linked to the online version of the paper at http://www.nature.com/jid

REFERENCES

Al-Daraji WI, Grant KR, Ryan K *et al.* (2002) Localization of calcineurin/NFAT in human skin and psoriasis and inhibition of calcineurin/NFAT activation in human keratinocytes by cyclosporin A. *J Invest Dermatol* 118:779–88

Anliker B, Chun J (2004) Cell surface receptors in lysophospholipid signaling. *Semin Cell Dev Biol* 15:457–65

Baker DL, Morrison P, Miller B *et al.* (2002) Plasma lysophosphatidic acid concentration and ovarian cancer. *JAMA* 287:3081–2

Balazs L, Okolicany J, Ferrebee M *et al.* (2001) Topical application of the phospholipid growth factor lysophosphatidic acid promotes wound healing *in vivo*. *Am J Physiol Regul Integr Comp Physiol* 280:R466–72

Bikle DD, Ratnam A, Mauro T *et al.* (1996) Changes in calcium responsiveness and handling during keratinocyte differentiation. Potential role of the calcium receptor. *J Clin Invest* 97:1085–93

Canning MT, Nay SL, Pena AV *et al.* (2006) Calcineurin inhibitors reduce nuclear localization of transcription factor NFAT in UV-irradiated keratinocytes and reduce DNA repair. *J Mol Histol* 37:285–91

Chow W, Hou G, Bendeck MP (2008) Glycogen synthase kinase 3beta regulation of nuclear factor of activated T-cells isoform c1 in the vascular smooth muscle cell response to injury. *Exp Cell Res* 314:2919–29

Corral RS, Iniguez MA, Duque J *et al.* (2007) Bombesin induces cyclooxygenase-2 expression through the activation of the nuclear factor of activated T cells and enhances cell migration in Caco-2 colon carcinoma cells. *Oncogene* 26:958–69

Demoyer JS, Skalak TC, Durieux ME (2000) Lysophosphatidic acid enhances healing of acute cutaneous wounds in the mouse. *Wound Repair Regen* 8:530–7

Dobrydneva Y, Williams RL, Blackmore PF (2010) Diethylstilbestrol and other nonsteroidal estrogens: novel class of store-operated calcium channel modulators. *J Cardiovasc Pharmacol* 55:522–30

Dolmetsch RE, Lewis RS, Goodnow CC *et al.* (1997) Differential activation of transcription factors induced by Ca^{2+} response amplitude and duration. *Nature* 386:855–8

Eichholtz T, Jalink K, Fahrenfort I *et al.* (1993) The bioactive phospholipid lysophosphatidic acid is released from activated platelets. *Biochem J* 291(Part 3):677–80

Flockhart RJ, Armstrong JL, Reynolds NJ *et al.* (2009) NFAT signalling is a novel target of oncogenic BRAF in metastatic melanoma. *Br J Cancer* 101:1448–55

Flockhart RJ, Diffey BL, Farr PM *et al.* (2008) NFAT regulates induction of COX-2 and apoptosis of keratinocytes in response to ultraviolet radiation exposure. *FASEB J* 22:4218–27

Frischauf I, Schindl R, Derler I *et al.* (2008) The STIM/Orai coupling machinery. *Channels (Austin)* 2:261–8

Goetzl EJ, An S (1998) Diversity of cellular receptors and functions for the lysophospholipid growth factors lysophosphatidic acid and sphingosine 1-phosphate. *FASEB J* 12:1589–98

Gwack Y, Feske S, Srikanth S *et al.* (2007) Signalling to transcription: store-operated $Ca2+$ entry and NFAT activation in lymphocytes. *Cell Calcium* 42:145–56

Hampton PJ, Jans R, Flockhart RJ *et al.* (2012) Lithium regulates keratinocyte proliferation via glycogen synthase kinase 3 and NFAT2 (nuclear factor of activated T cells 2). *J Cell Physiol* 227:1529–37

Hirano K, Hirano M, Hanada A (2009) Involvement of STIM1 in the proteinase-activated receptor 1-mediated $Ca2+$ influx in vascular endothelial cells. *J Cell Biochem* 108:499–507

Horsley V, Aliprantis AO, Polak L *et al.* (2008) NFATc1 balances quiescence and proliferation of skin stem cells. *Cell* 132:299–310

Inoue M, Kratz G, Haegerstrand A *et al.* (1995) Collagenase expression is rapidly induced in wound-edge keratinocytes after acute injury in human skin, persists during healing, and stops at re-epithelialization. *J Invest Dermatol* 104:479–83

Jans R, Atanasova G, Jadot M *et al.* (2004) Cholesterol depletion upregulates involucrin expression in epidermal keratinocytes through activation of p38. *J Invest Dermatol* 123:564–73

Jauliac S, Lopez-Rodriguez C, Shaw LM *et al.* (2002) The role of NFAT transcription factors in integrin-mediated carcinoma invasion. *Nat Cell Biol* 4:540–4

Jones BF, Boyles RR, Hwang SY *et al.* (2008) Calcium influx mechanisms underlying calcium oscillations in rat hepatocytes. *Hepatology* 48:1273–81

Liao Y, Erxleben C, Abramowitz J *et al.* (2008) Functional interactions among Orai1, TRPCs, and STIM1 suggest a STIM-regulated heteromeric Orai/TRPC model for SOCE/Icrac channels. *Proc Natl Acad Sci USA* 105:2895–900

Liao Y, Erxleben C, Yildirim E *et al.* (2007) Orai proteins interact with TRPC channels and confer responsiveness to store depletion. *Proc Natl Acad Sci USA* 104:4682–7

Lichte K, Rossi R, Danneberg K *et al.* (2008) Lysophospholipid receptor-mediated calcium signaling in human keratinocytes. *J Invest Dermatol* 128:1487–98

Macian F (2005) NFAT proteins: key regulators of T-cell development and function. *Nat Rev Immunol* 5:472–84

Magee AI, Lytton NA, Watt FM (1987) Calcium-induced changes in cytoskeleton and motility of cultured human keratinocytes. *Exp Cell Res* 172:43–53

Mammucari C, Tommasi di Vignano A, Sharov AA *et al.* (2005) Integration of Notch 1 and calcineurin/NFAT signaling pathways in keratinocyte growth and differentiation control. *Dev Cell* 8:665–76

Martin AC, Willoughby D, Ciruela A *et al.* (2009) Capacitative $Ca2+$ entry via Orai1 and STIM1 regulates adenylyl cyclase type 8. *Mol Pharmacol* 75:830–42

Mazereeuw-Hautier J, Gres S, Fanguin M *et al.* (2005) Production of lysophosphatidic acid in blister fluid: involvement of a lysophospholipase D activity. *J Invest Dermatol* 125:421–7

Noguchi K, Herr D, Mutoh T *et al.* (2009) Lysophosphatidic acid (LPA) and its receptors. *Curr Opin Pharmacol* 9:15–23

Potier M, Gonzalez JC, Motiani RK *et al.* (2009) Evidence for STIM1- and Orai1-dependent store-operated calcium influx through ICRAC in vascular smooth muscle cells: role in proliferation and migration. *FASEB J* 23:2425–37

Roedding AS, Li PP, Warsh JJ (2006) Characterization of the transient receptor potential channels mediating lysophosphatidic acid-stimulated calcium mobilization in B lymphoblasts. *Life Sci* 80:89–97

Ross K, Parker G, Whitaker M *et al.* (2008) Inhibition of calcium-independent phospholipase A impairs agonist-induced calcium entry in keratinocytes. *Br J Dermatol* 158:31–7

Ross K, Whitaker M, Reynolds NJ (2007) Agonist-induced calcium entry correlates with STIM1 translocation. *J Cell Physiol* 211:569–76

Sage SO, Merritt JE, Hallam TJ *et al.* (1989) Receptor-mediated calcium entry in fura-2-loaded human platelets stimulated with ADP and thrombin. Dual-wavelengths studies with Mn2+. *Biochem J* 258:923–6

Santini MP, Talora C, Seki T *et al.* (2001) Cross talk among calcineurin, Sp1/Sp3, and NFAT in control of p21(WAF1/CIP1) expression in keratinocyte differentiation. *Proc Natl Acad Sci USA* 98:9575–80

Sauer B, Vogler R, Zimmermann K *et al.* (2004) Lysophosphatidic acid interacts with transforming growth factor-beta signaling to mediate keratinocyte growth arrest and chemotaxis. *J Invest Dermatol* 123:840–9

Schindl R, Bergsmann J, Frischauf I *et al.* (2008) 2-aminoethoxydiphenyl borate alters selectivity of Orai3 channels by increasing their pore size. *J Biol Chem* 283:20261–7

Schlondorff JS, Del Camino D, Carrasquillo R *et al.* (2009) Trpc6 mutations associated with focal segmental glomerulosclerosis cause constitutive activation of Nfat-dependent transcription. *Am J Physiol Cell Physiol* 296:C558–69

Sekharam M, Cunnick JM, Wu J (2000) Involvement of lipoxygenase in lysophosphatidic acid-stimulated hydrogen peroxide release in human HaCaT keratinocytes. *Biochem J* 346(Part 3):751–8

Thebault S, Flourakis M, Vanoverberghe K *et al.* (2006) Differential role of transient receptor potential channels in Ca2+ entry and proliferation of prostate cancer epithelial cells. *Cancer Res* 66:2038–47

Todd C, Reynolds NJ (1998) Up-regulation of p21WAF1 by phorbol ester and calcium in human keratinocytes through a protein kinase C-dependent pathway. *Am J Pathol* 153:39–45

Tu CL, Chang W, Bikle DD (2001) The extracellular calcium-sensing receptor is required for calcium-induced differentiation in human keratinocytes. *J Biol Chem* 276:41079–85

Tu CL, Oda Y, Komuves L *et al.* (2004) The role of the calcium-sensing receptor in epidermal differentiation. *Cell Calcium* 35:265–73

Vassilieva EV, Gerner-Smidt K, Ivanov AI *et al.* (2008) Lipid rafts mediate internalization of beta1-integrin in migrating intestinal epithelial cells. *Am J Physiol Gastrointest Liver Physiol* 295:G965–76

Wilkins BJ, Dai YS, Bueno OF *et al.* (2004) Calcineurin/NFAT coupling participates in pathological, but not physiological, cardiac hypertrophy. *Circ Res* 94:110–8

Yang S, Zhang JJ, Huang XY (2009) Orai1 and STIM1 are critical for breast tumor cell migration and metastasis. *Cancer Cell* 15:124–34

Zakharov SI, Smani T, Dobrydneva Y *et al.* (2004) Diethylstilbestrol is a potent inhibitor of store-operated channels and capacitative Ca(2+) influx. *Mol Pharmacol* 66:702–7

Zarayskiy V, Monje F, Peter K *et al.* (2007) Store-operated Orai1 and IP3 receptor-operated TRPC1 channel. *Channels (Austin)* 1:246–52

Zuo W, Chen YG (2009) Specific activation of mitogen-activated protein kinase by transforming growth factor-beta receptors in lipid rafts is required for epithelial cell plasticity. *Mol Biol Cell* 20:1020–9